Realistic mobility simulation of urban mesh networks ☆

Jonghyun Kim, Vinay Sridhara, Stephan Bohacek *

Department of Electrical and Computer Engineering, University of Delaware, Newark, DE 19716, United States

ABSTRACT

It is a truism that today's simulations of mobile wireless networks are not realistic. In realistic simulations of urban networks, the mobility of vehicles and pedestrians is greatly influenced by the environment (e.g., the location of buildings) as well as by interaction with other nodes. For example, on a congested street or sidewalk, nodes cannot travel at their desired speed. Furthermore, the location of streets, sidewalks, hallways, etc. restricts the position of nodes, and traffic lights impact the flow of nodes. And finally, people do not wander the simulated region at random, rather, their mobility depends on whether the person is at work, at lunch, etc. In this paper, realistic simulation of mobility for urban wireless networks is addressed. In contrast to most other mobility modeling efforts, most of the aspects of the presented mobility model and model parameters are derived from surveys from urban planning and traffic engineering research. The mobility model discussed here is part of the UDel Models, a suite of tools for realistic simulation of urban wireless networks. The UDel Models simulation tools are available online.

© 2008 Elsevier B.V. All rights reserved.

1. Introduction

By providing connectivity to mobile users, mesh networks are poised to become a major extension of the Internet. More than 300 cities and towns have plans to deploy mesh networks, and several dozen cities have already deployed mesh networks [1]. While some deployments have been in smaller cities, such as Mountain View, CA and St. Cloud, FL, some deployments have been in larger cities such as Corpus Christi's 147 sq. mile deployment [2] and Philadelphia's 131 sq. mile deployment. These mesh networks are meant to enhance city and emergency services communication as well as to provide city-wide, low-cost, ubiquitous Internet access for residents and visitors. Such

networks promise to bring dramatic changes to data accessibility and hence have a major impact on society.

While mesh networks have much promise, there are important issues regarding performance and scalability that have yet to be resolved. However, the lack of realistic simulators stymies the development and testing of new protocols for large-scale urban mesh networks (LUMNets).

While researchers have extensively studied the simulation of wired networks, the influence of propagation and mobility on LUMNet performance requires new efforts in simulation. To further motivate the need for mobility and propagation simulation, consider the problem of mobility management for LUMNets (which is necessary for scalability). As is the case for mobile phone networks [3–7], there are many mobility management techniques that network designers could apply to LUMNets. However, node mobility and the propagation range of base stations greatly influence the performance of these schemes. For example, small indoor coverage areas, may result in rapid node migration, whereas large outdoor coverage areas result in slower node migration when the node is a walking person, but more rapid migration when the person is in a car. The fact that some base stations will have coverage that extends both indoors

and outdoors further complicates mobility management. See [8] for an example where the propagation characteristics of an urban area are exploited for efficient mobility management. Beyond mobility management, propagation and mobility are also known to have a considerable impact on the performance of TCP [9,10], routing [11–15], MAC [16], and the physical layer [17].

While researchers have previously examined realistic propagation (e.g., see [18] and references therein), realistic mobility has received less attention. The approach to realistic mobility models described in this paper is significantly different from other mobility models in that much of the model is based on surveys. Specifically, the simulator uses surveys on time use from the US Bureau of Labor Statistics, and an extensive set of surveys of pedestrian and vehicle mobility developed within Urban Planning (e.g. [19,20]). Furthermore, mobility within office buildings uses surveys from the meetings analysis research area. It should be stressed, that the mobility model is not ad hoc, but is based on the findings of mature research communities. For example, Time Use Studies has been active for approximately 40 years [21] and many aspects of the agent mobility (see Section 4 for definition), have been known for 30 years and are integrated into government guidelines on traffic planning [20]. This paper distills the results of these areas and presents the aspects that are important for urban mobility.

Another novel aspect of the model is that it is comprehensive in that it supports many different types of urban mobility, including indoor mobility, outdoor pedestrian, and outdoor vehicle mobility. The model also accounts for the time-of-day. Consequently, city-wide simulations are possible. The mobility model presented in this paper is part of a suite of freely available tools for simulating urban wireless networks known the UDel Models [22]. Besides the UDel Mobility Model, the UDel Models includes a tool for computing realistic propagation as well as several tools for processing data and making city maps. The web-site also includes example data sets such as mobility traces and propagation traces.

The remainder of the paper proceeds as follows. In the next section, an overview of the simulation of urban networks is presented. Section 3 discusses techniques for developing city maps. Clearly, mobility and propagation are greatly affected by the map. Section 4 presents the mobility model of people. This model has three parts, namely, the activity model, the task model, and the agent model. These models are discussed in Sections 4.1, 4.3, and 4.4, respectively. Section 4.5 provides some details on how commuting is implemented, while Section 4.6 discusses how realistic population sizes can be determined. Section 5 presents a model for car mobility. Section 6 validates the model against real date. Section 7 investigates the impact that realistic mobility models have on network performance. Related work on mobility modeling is provided in Section 8. Then future directions in realistic mobility modeling are discussed in Section 9 and concluding remarks are made in Section 10.

2. Mobile wireless network simulation overview

There are several stages to LUMNet simulation. The first step is to define the simulated city map. This step is dis-

cussed in Section 3. The second step is to determine the propagation matrix for the simulated region. The propagation matrix includes characteristics such as the channel gain, delay spread, and angle of arrival for each possible transmitter–receiver pair in the simulated region. Simulating urban propagation is discussed in [18]. Next, the city map and a mobility model are used to generate one or more mobility trace files. Realistic urban mobility is the focus of this paper. From the mobility trace file and the propagation matrix, the propagation trace file is computed; the propagation trace file provides the channel model between all pairs of nodes at every moment of the simulation. Protocol simulators such as QualNet, ns-2, or OPNET use the propagation and mobility trace files.

3. City maps

In order to simulate an urban wireless network, it is necessary to model the urban geography. There are several ways that maps for simulation can be developed. The algorithm described in [23] places buildings at random and uses Voronoi diagram to construct sidewalks between the buildings. One drawback of such an approach is that important aspects of cities such as long thoroughfares and big intersections are neglected. It is well known that streets play an important role in mobile phone communication and it has been shown that streets play an important role in connectivity in MANETs [24].

A more realistic way to generate cities is to utilize detailed GIS data sets [25]. These data sets include 3-dimensional maps of buildings that provide enough detail for realistic simulation. There are a large number of such data sets. For example, there are GIS data sets for most American cities. The UDel Models map building suite of tools converts GIS data sets into format suitable for a specialized graphical editor. The UDel Models also includes a graphical editor to "touch-up" the GIS map (e.g., remove spurious buildings). The editor is also allows one to add roads, sidewalks, traffic lights, base stations, subway stations, define the types of buildings (e.g., residence, store/restaurant, office), and define building materials (building materials impact propagation [18]). While GIS data sets have details of building heights and position, they typically do not provide details about the interiors of the building. In lieu of actual interiors, they must be automatically generated. The UDel Models uses layouts shown in Fig. 1.

Another realistic method to generate city maps is to use US Census Bureau's TIGER data (Topologically Integrated Geographic Encoding and Referencing) [26]. The TIGER data includes roads, railroads, rivers, lakes, and legal boundaries in the US. It also contains information about roads including their location in latitude and longitude, name, type, address ranges, and speed limits. However, it does not include information about buildings. TIGER data is often used for realistic maps for simulating vehicle ad hoc networks [27–29].

In general, nodes (people or vehicles) may be at a large number of locations within the city. However, restricting node movements to a specific graph, results in a significant computational savings. The UDel Models define a large set
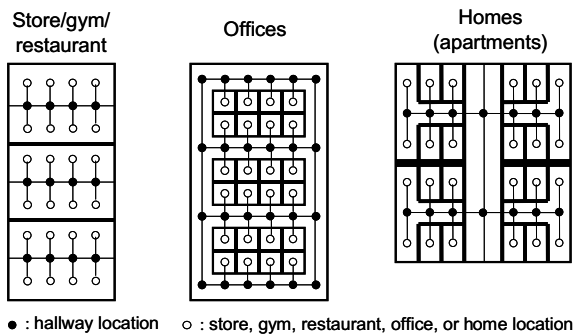
Fig. 1. Locations in different types of buildings. Locations are marked with a circle while arcs are indicated by thin lines. The thick lines denote walls. The store/gym/restaurant structure is such that each third of the layout can be any of these options. The apartment building shown has four apartments each with five rooms. The size and number of rooms depends on the building size.

of locations (vertices) and pathways (arcs). Examples of parts of this graph are shown in Fig. 1.

4. Mobility of people

This section presents a detailed mobility model of urban pedestrians during the workday. This model utilities three mature research areas, namely, urban planning [19,20], meeting analysis [30], and use of time [21]. The resulting model is a three layer hierarchical model. The top layer is the activity model that determines high-level types of activities, the time when people start and end the activities as well as the location where the activity is performed. Such models are sometime referred to as macro-mobility models [31]. To develop this model, we used data from the 2003 US Bureau of Labor Statistics (BLS) use of time study [32]. This study includes interviews with roughly 20,000 people. Furthermore, the BLS determined weightings to account for over sampling of some types of people (e.g., unemployed people tend to be at home at the time of the interview call and tend to be oversampled). Hence, the significance of the study exceeds the 20,000 that were actually interviewed. This study collected detailed data on the activities performed by interviewee including the times that activities were started and stopped, where the activities were performed, and for what reason the activity was performed.

The second layer of the pedestrian mobility model is the task model. While performing a particular activity, a person may carry out many tasks. For example, the model discussed here focuses on office workers. While such nodes are performing a work activity, there are two possible tasks, namely, working at their desk, and meeting with other workers. The basis of this part of the mobility model is several seminal studies of worker meetings performed within the management research community (see [30] and references therein). This part of the model allows one to determine how nodes move within a building and how nodes are clustered within buildings. Mobility within buildings is important if networks utilize relaying by mobile nodes. For example, an outdoor network such as Philadelphia's can greatly increase its indoor coverage if mobile nodes

can act as relays [33]. To determine the performance of such relaying, the mobility of indoor nodes must be modeled.

The third layer of the mobility model is the agent model and defines how nodes navigate walkways to their desired destinations. This model is based on urban planning research, especially the seminal work of Pushkarev and Zupan [19] as well as several other pedestrian mobility studies. A key feature of this part of the mobility model is that it realistically models how nodes form clusters or platoons. Such clusters are important since nodes in close proximity will experience strong interference. On the other hand, presence of clusters of nodes enhances the formation of ad hoc or virtual antenna arrays. For these reasons, the model includes several mechanisms that impact platooning.

4.1. Activity model

This part of the mobility model is based on the US Bureau of Labor Statistics (BLS) 2003 time use study [32]. This study identifies a large number of activities. We focus on those activities that indicate location, and group together activities that are performed in the same location (e.g., all activities performed at home are grouped together into the *at home* activity). While the BLS study also collected coarse location information, this modeling effort used both activity and location information to determine the location. We focus on eight types of activities: working, eating not at work, shopping, at home, receiving professional service, exercise, relaxing, and dropping off someone. Note that since we focus on location and mobility, eating at work is counted as work. Eating not at work includes eating at a restaurant and buying food somewhere besides at work. Shopping includes all types of shopping except buying food. Receiving professional service ranges from things such as getting medical attention to receiving household management and maintenance services that are not performed at home.

During the simulation initialization, each node is given an office and home. We assume that work is done within the building where the nodes office is located (work done at home is included into the at home activity), eating is done at a restaurant (eating at home is included into at home activity), shopping is done at a randomly selected store, and receiving professional service is done at an office that is not the node's office. We do not specify special locations for relaxing or dropping someone off. Dropping someone off includes meeting children at school and taking them home. For the purpose of mobility modeling, we model such activities as a trip home followed by a trip to a random selected office location. The node remains at the office location until the drop off activity if complete. The relaxing activity is modeled as going to an office location (much like receiving professional service).

This model focuses on the work day which consists of being at home, going to work, working, perhaps taking a break, leaving work, and returning home. The model neglects activities before and after work. Future work will include the rest of the day.

For each person, the following steps are taken to determine the activities that they perform.

(1) Select a home and office.
(2) Determine the arrival time at work.

(3) Determine the duration at work.
(4) Determine if a break from work is taken. (The next five steps assume a break is taken.)
(5) Determine the break start time.
(6) Determine the number of activities performed during a break.
(7) Determine which activities are performed during the break.
(8) Determine the duration of each activity.
(9) Determine the arrival time back at work and determine if a break is taken again. If so, steps 5–9 are repeated.

Selection of home and office. For each simulated person, an office is selected at random. Once an office is selected, a home is selected that is nearby the office. In case the person does not live in the city (the fraction of people that live within the city depends on the amount of residential area), then the person enters the city by subway or by car. In such cases, instead of assigning the person a home, they are assigned a parking lot or a subway stop. The home, parking lot, and subway stops are selected so that the distance to the office matches the distribution shown in Fig. 2, which shows the distribution of walking distances collected by Pushkarev and Zupan. Further discussion on the mode of travel to work can be found in Section 4.5.

Arrival time at work. Fig. 3 shows the empirical complementary cumulative distribution function (CCDF) of the time of arrival at work as found by the BLS survey. We modeled the surveyed values with a mixture of exponential and Gaussian distribution. Specifically, by minimizing the L^1 norm of the difference between the empirical probability density function (PDF) from the surveyed arrival times and the modeled distribution, we found that with probability of 0.552, the time of arrival is normally distributed with mean 7:46 a.m. and standard deviation of 45 min. Furthermore, we found that with probability (1–0.552), the time of arrival is exponentially distributed with the mean time of arrival of 12:00. We shifted the exponential distribution so that the earliest minimum time of arri-
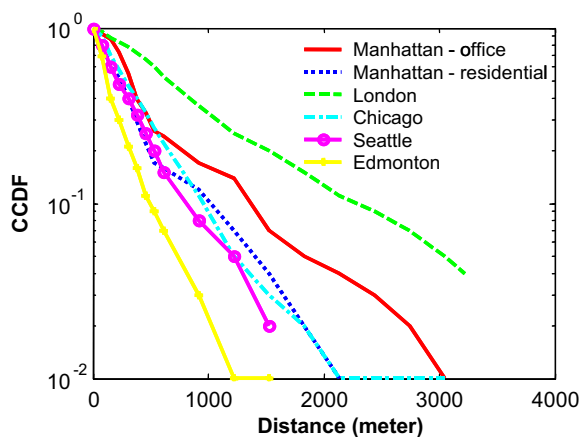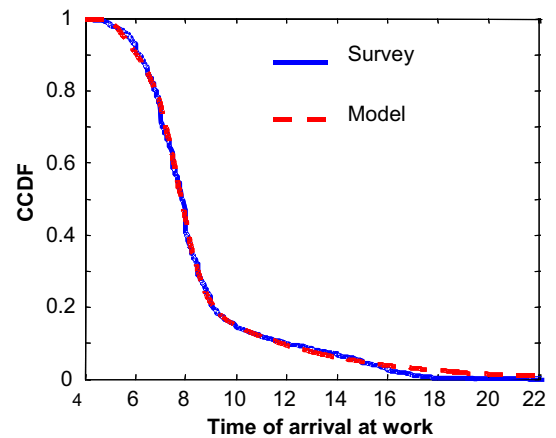

Fig. 3. The complimentary cumulative distribution function (CCDF) of the time of arrival at work.

val in this case is 5 a.m. Similarly, we truncated the normal distribution so that no arrivals occur before 5 a.m.

Duration at work. Fig. 5 shows the empirical CCDF of the duration at work for people that arrive at work between 7 and 8 in the morning and for those that arrive between 10 and 11 in the morning as found by the BLS survey. Using the L^1 norm of the difference between the empirical PDF and the PDF of the model as a measure of the quality of fit, we modeled these distributions and ones for other arrival times at work with a mixture of a normal random variable and an exponential random variable. These distributions have four parameters, α, the probability of selecting the normal distribution, μ and σ the mean and the standard deviation of the normal distribution, and m, the mean of the exponential distribution. Table 1 shows the value of these parameters for the different arrival times at work. Surprisingly, while the model is simple, the fit shown in Fig. 5 is a typical quality of fit throughout the day. On the other hand, from Fig. 3 it can be seen that the most important distribution is for nodes arriving between 7 and 8.

Whether a break is taken. The probability of whether a break is taken depends on the time of arrival at work. Note that if a break is not taken, the person may still eat lunch, but they do not leave the building. We modeled the probability of taking a break conditioned on the time of arrival with a piece-wise linear function of the time of arrival. In this case, the fit was by eye, that is, we adjusted the parameters until

Fig. 2. CCDF of distance traveled during outdoor walking trips. This data is from [19].

Table 1
Duration at work model parameters

Time	α	μ	σ	m
⩽8 a.m.	0.91	8:09	1:06	9:50
8–9	0.85	7:49	0:56	8:52
9–10	0.81	7:16	1:17	5:52
10–11	1.0	7:11	2:16	–
11–12	0.70	7:16	2:11	5:00
12–1	1.0	6:19	2:40	–
1–3	0.5	7:33	0:55	4:31
3–6	0.83	6:18	1:55	2:07
⩾6	1.0	4:30	2:26	–
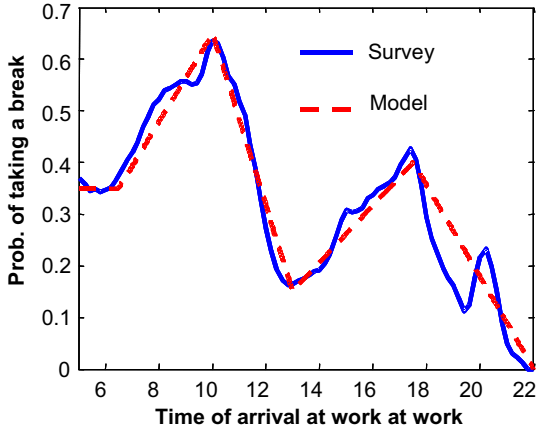
Fig. 4. The probability of taking a break given the arrival time at work.

Fig. 6. The rate that a person takes a break and leaves work given the current time. Also shown are the rates conditioned on the person being at work for at least 1 and 2 h. These rates are within the 90% confidence intervals that are also shown. Finally, the fitted rate is also shown.

the piece-wise linear function approximated the data from the survey

P(taking a break|arrival time at work $= t$)

$$= \begin{cases} 0.35 & \text{for } t < 6.5, \\ 0.86(t - 6.5) + 0.35 & \text{for } 6.5 \leqslant t \leqslant 10, \\ 0.17(t - 10) - 0.65 & \text{for } 10 \leqslant t \leqslant 13, \\ 0.056(t - 13) + 0.15 & \text{for } 13 \leqslant t \leqslant 17.5, \\ -0.08(t - 17.50) + 0.4 & \text{for } t \geqslant 17.5. \end{cases}$$

Note that this equation uses fraction of hours past midnight, not hours and minutes. Fig. 4 shows the modeled and the surveyed probability.

The time the break is started. Clearly, one cannot go on a break before they arrive at work. However, once they arrive at work, the rate that a person goes on a break does not significantly depend on how long they have been at work. Fig. 6 shows this rate conditioned on the person arriving at work at least one hour ago, conditioned on the person arriving at work at least two hours ago, and unconditionally. Observed that the duration at work has only a minor impact on the time to take a break and that
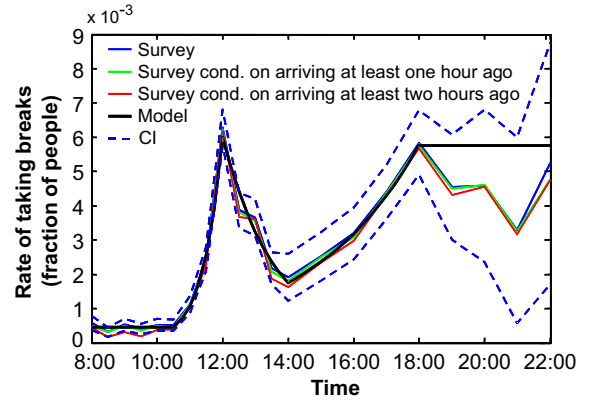
this difference is within the 90% confidence intervals. Thus, we assume that the rate of going on a break is independent of the arrival time, assuming that the node has already arrived at work. The rate that a person takes a break is approximated by

$$r(t) = \begin{cases} 0.004 & \text{for } t < 10.5, \\ 0.006 \times \exp(-1.7(12 - t)) & \text{for } 10.5 \leqslant t \leqslant 12, \\ 0.006 \times \exp(-0.6(t - 12)) & \text{for } 12 \leqslant t \leqslant 14, \\ 0.0058 \times \exp(-0.3(5 - t)) & \text{for } 14 \leqslant t \leqslant 18, \\ 0.0058 & \text{for } t > 18. \end{cases}$$

(1)

By rate of taking a break, we mean that the probability that a node will take a break within the time interval from t_0 to t_1 is $(t_1 - t_0) \int_{t_0}^{t_1} r(\tau) d\tau$. The parameters used in (1) were found as follows. As can be observed in Fig. 6, the rate of taking a break as a function of time has five regions, namely $t < 10.5$, $10.5 \leqslant t \leqslant 12$, $12 \leqslant t \leqslant 14$, $14 \leqslant t \leqslant 18$,
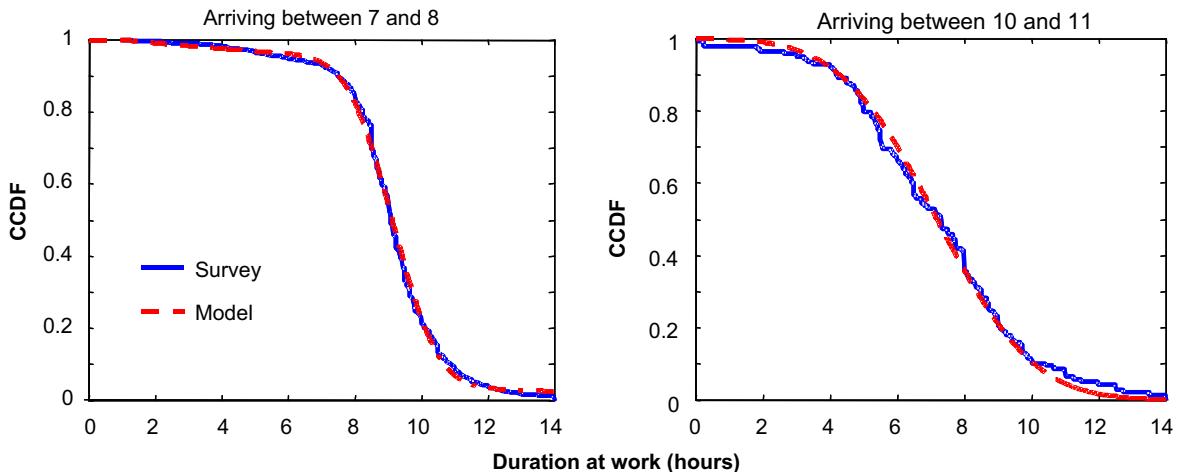

Fig. 5. The CCDF of the duration at work for two different arrival times at work.

and $t > 18$. During the first region, the rate is approximately constant, thus we model the rate during this period as a constant rate equal to 0.004, which is the average rate observed during this period. Relatively few of the BLS interviewees were at work after 6 p.m., and hence the confidence interval during this period is large. Hence, we simply model the rate of taking breaks as a constant rate equal to 0.0058, which is the surveyed rate at 6 p.m.. The three periods between 10:30 a.m. and 6 p.m. appear to be polynomial or exponential. Thus, we assumed that the rates vary exponentially and modeled these exponential curves to minimize the L^1 error between the modeled rate and surveyed rate. The optimization was constrained so rate is continuous.

Number of activities performed during a break. Fig. 7 shows the probability of performing different numbers of activities during a break, as collected by the BLS survey. We see that over the course of the day, the number of activities performed varies. However, the variation is small, and hence we model the probability to be independent of the time of day. The model probabilities are shown in Fig. 7. We selected these probabilities by averaging over all surveyed breaks in the BLS data.

Which activities are performed during a break. The types of activities performed during a break strongly depend on the number of activities to be performed. Fig. 7 shows the fraction of breaks that include the indicated activity. This data is directly from the BLS survey. We do not model these probabilities, but use them directly in the mobility model. Note that if a person performs more than one activity, the fractions sum to more than one.

Duration of activities. The time spent performing an activity depends on the type of activity. Fig. 8 shows the CCDF of the duration of three activities as found by the BLS survey. The distribution of the duration of eating shows a jump at 1 h. Smaller jumps are noticeable in the distribution of other activities. We modeled the duration of these and the other activities as a mixture of an exponentially distributed random variable conditioned on the duration being larger than a minimum duration along with deterministic duration of one hour. Thus, the distribution of the duration of each activity has three parameters, μ, the mean of the exponential distribution, $\underline{d}$, the minimum duration, and ρ, the probability of the duration lasting exactly one hour. Table 2 shows the values of the model parameters for the different activities considered. These parameters were found by minimizing the L^1 norm of the different of the empirical PDF found from the BLS survey and the modeled PDF.

Location of activity. Once the activity has been selected, the location of the activity must be determined. Specifically, eating requires selecting a restaurant, exercising requires selecting a gym, getting professional service requires selecting an office location, shopping requires selecting a store, dropping someone off requires selecting an office location to drop them off at. We assume that people walk to the location that is required to perform the activity. Future work will include the case where people take other forms of transportation. Through observation, Pushkarev and Zupan [19] found the distribution of the distance that pedestrians walk shown in Fig. 2. Since the relationship between probability and the distance walked is approximately linear on a semilog plot, we conclude that the distance is well modeled by an exponential distribution. We found that the mean distance to be 554 m, 380 m, 403 m, 344 m, 813 m, and 216 m for Manhattan from office buildings, Manhattan from residences, Chicago, Seattle, London and Edmonton, respectively. We see that the US cities have approximately the same mean. Thus, we select a location of the correct type (e.g., a store for shopping) at random such that the walking distance is exponentially distributed with mean 400 m.

4.2. Activity model of people who did not work

On a particular work day, the BLS estimates that about 8% of people did not work. Of these, about 30% did not take any trips. Thus, the fraction of pedestrians that are not

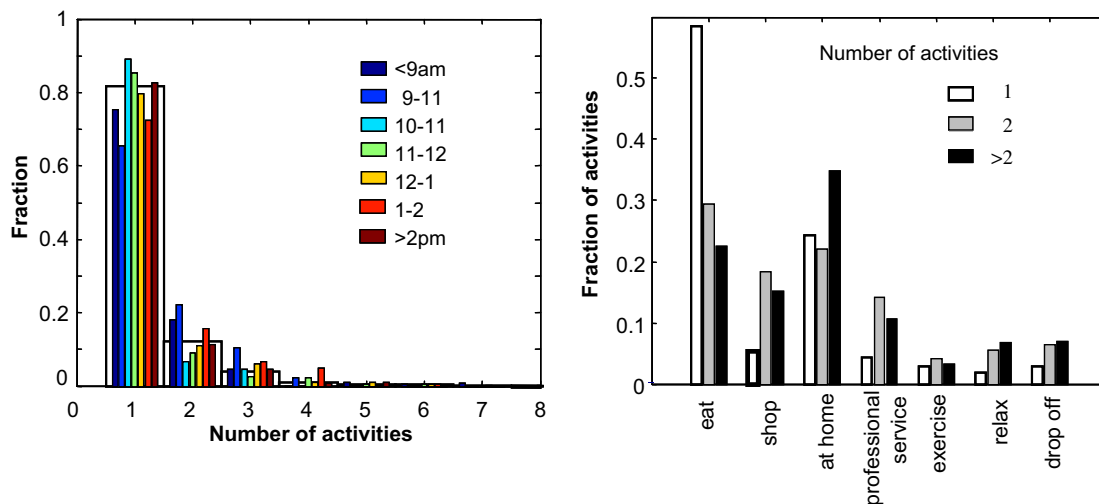

Fig. 7. Left: the number of activities done during a break conditioned on the time that the break is started. Right: the fraction of time that a break includes the indicated activity given the number of activities performed within the break.
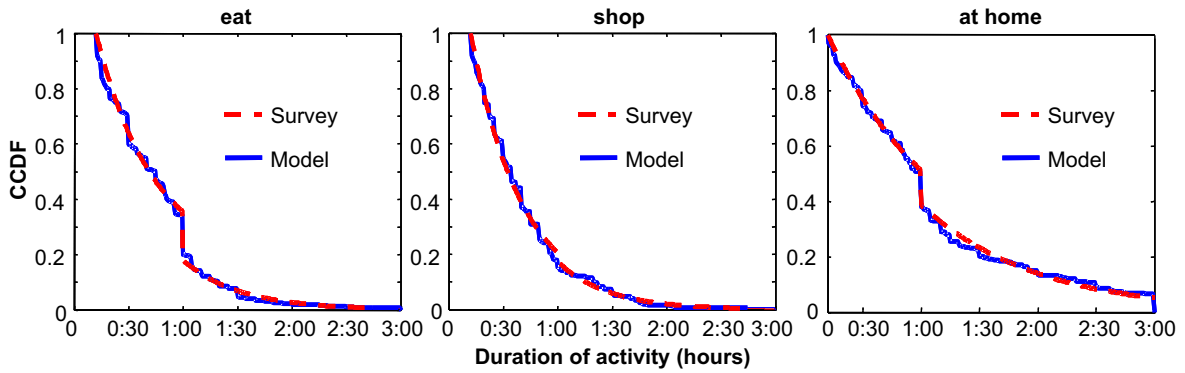
Fig. 8. CCDF of the duration of eat, shop, and at home activities.

Table 2
Duration of activity model parameters

Activity	μ	$\underline{d}$	ρ
Eat	0:31	0:20	0.18
Shop	0:28	0:20	0.03
At home	1:00	0:20	0.12
Professional	0:44	0:10	0.04
Exercise	0:35	0:20	0
Relax	0:27	0:15	0.01
Drop-off	0:19	0:10	0.02

working is approximately 5.6%. Since this fraction is so small, a detailed model is not justified. Instead, we propose the following simple model. Nonworkers make a series of excursions where the probability of taking the next excursion is 0.7. Thus, the number of excursions taken is geometrically distributed. Quality of fit of this model is shown in Fig. 9.

We assume that each excursion takes the pedestrian to a random office in the simulated city where the destination is selected so that the distance to the destination is exponentially distributed, as discussed in Section 4.1. Upon arriving at the destination, the node remains at the location for an exponentially distributed amount of time with mean 1.07 h. The quality of fit of this model is shown in Fig. 10.

Mimicking the time of arrival at work described in Section 4.1, we model that the sequence of excursions starts at a time whose distribution is a mixture of an exponential random variable and a normally distributed random variable. Specifically, with probability 0.17, the distribution of the start time of the first excursion is exponential with mean 6 p.m., and with probability 0.83, the start time is normally distributed with mean 10 a.m. and standard deviation of 3 h. This model and the empirical CCDF from the BLS survey are shown in Fig. 11.

4.3. Task model

Some activities consist of a single task. For example, eating consists of going to a restaurant. However, shopping and working consist of multiple tasks. We model shopping as a simple random walk inside the store. However, this

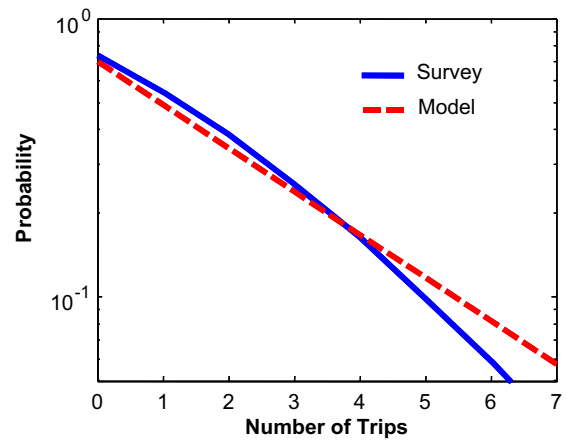Fig. 9. Empirical CCDF of the number of excursions taken by nonworkers and the fitted geometric CCDF with parameter $p = 0.3$.
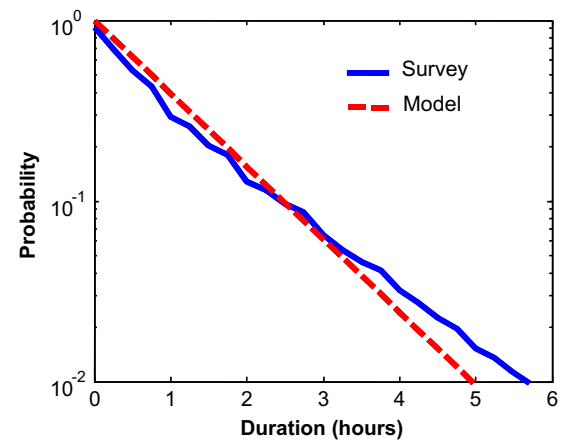

Fig. 10. Empirical CCDF of the duration of an excursion and the fitted exponential geometric CCDF with parameter $\mu = 1.07$ h.

model is based on intuition; future work is required to verify this model. The work activity is modeled in a more complicated manner that focuses on modeling meetings.
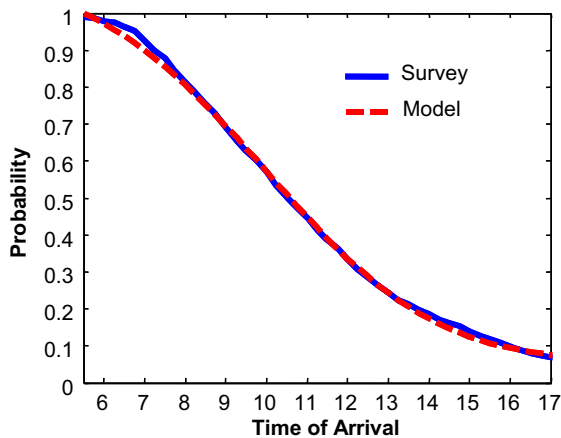
Fig. 11. Empirical CCDF of the start time of a nonworkers series of excursions and the CCDF of the model.

Table 3
Meetings model parameters

Meeting size	Mean duration	Probability
2	21 (min)	0.65
3	19	0.12
4	57	0.04
5	114	0.02
6	37	0.04
7	50	0.03
8	150	0.01
9	75	0.02
10	150	0.01
15	30	0.025
20	30	0.025

Specifically, [30,34,35] have collected data on the frequency, size, and durations of meetings; [34] includes two person meetings. These studies allow the model to include worker interactions. Thus, we model mobility while at work as a sequence of meetings followed by working in the node's office. This process repeats until the work activity is complete.

More specifically, meetings are simulated as follows. We assumed that the time between meetings is exponentially distributed. When a meeting begins, a random number of people are selected to attend the meeting. Based on the number of people attending, the mean duration of the meeting is determined. We assumed that the duration is exponentially distributed. While the assumptions that these time durations are exponential are merely a simplifying modeling assumptions, the exponential and closely related Poisson distribution have been shown to be good models when modeling the occurrences of events [36].

The model parameters are the mean time between meetings, the distribution of the size of meetings, and the relationship between number of meeting participants and the mean meeting duration. These parameters are derived from [30,34,35]. Specifically, the mean time between meetings is 18 min while Table 3 gives the remaining of the model parameters.

4.4. Agent model – node dynamics and interactions

This part of the model is known as the agent model and is responsible for determining the trajectory of the node as it moves from one location to the next. Models that focus on this type of mobility are known as micro-mobility models and agent models are a particular class of such models. We assume that nodes follow a path of hallways and sidewalk that make up a shortest path between the origin of the trip and the destination.[1] Hence high-level path finding is not an important part of the agent model. Rather, the agent model focuses on the dynamics and interaction between moving nodes. More specifically, the agent model consists of enforcing a distance–speed relationship between nodes and lane changing rules. The next two sections discuss these models. In Section 6.3, the model is validated by comparing the size of platoons created by the model to those observed by Pushkarev and Zupan. As will be discussed in Section 5, with some small changes, the node interactions described here are also applicable to vehicles.

#### 4.4.1. Inter-node distance–speed relationship

The distance–speed relationship is a critical aspect of node mobility. This relationship dictates that node move at a slower speed when they are more density packed (i.e. high density), and will only achieve high speed if node density is low. Since the node speed plays an important role in the performance of mesh networks, realistic mobility modeling requires a realistic model of the distance–speed relationship. We base the model developed in this section on the findings of urban planning researchers, who have extensively studied these relationships for both vehicle and pedestrian mobility.

Older and Navier were among the first to study the distance–speed relationship for pedestrians [37,38]. Fig. 12 shows the distance–speed relationship derived from their observations.[2] We approximate this relationship with $D(S) = S^{*}D_{min}/(1.08 \times S^{*} - S)$, where D_{min} is the minimum acceptable distance between people and S^{*} is the desired speed of the pedestrian. Pushkarev and Zupan found D_{min} to be at least 0.35 m [19], which is the valued used here. Fig. 12 shows the our model of the distance–speed relationship, where the desired speed S^{*} is the average speed observed at the lowest pedestrian density of one pedestrian per five meters. We selected the parameter 1.08 such that the desire speed is reached at a density of one pedestrian per 5 m.

As Fig. 12 shows, the desired speed of students is higher than the desired speed of a random sample of urban pedestrians. Instead of attempting to model the desired speed based characteristics such as age, we use the findings of Helbing and model the desired speed as Gaussian with mean 1.34 m/s and standard deviation 0.26 m/s [40–42].

---

[1] Due to the large number of possible destinations, a hierarchical scheme is used to find paths. This scheme is similar to hierarchical routing.

[2] The plot shown is based on area–speed relationships with the assumption of 0.75 m of lateral space between people as found by Oeding [39].
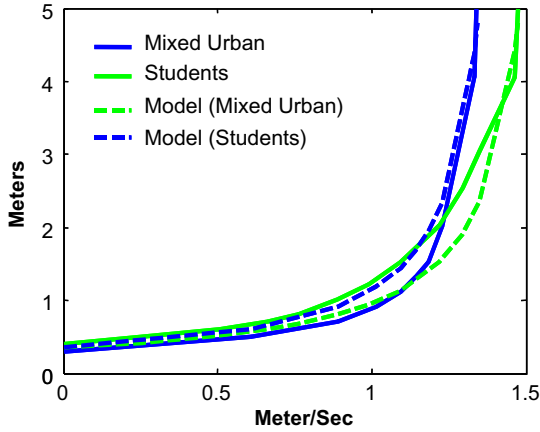
Fig. 12. Speed–distance relationship for pedestrians. The mixed urban pedestrian data is adapted from [37] and the student observations are adapted from [38].

4.4.2. Lane changing

Urban planners have recognized that lane changing plays an important role in node dynamics (see, for example [19,43]). Specifically, it has been observed that in the cases of pedestrians and vehicles, when a faster moving node catches up to a slower moving node, the faster moving node does not necessarily pass, but might simply adjust its speed to that of the slower node and follow the slower node. This lack of passing is one of the causes of clustering of nodes [19,43]. Section 6.3 discusses clustering in more detail.

While the dynamics of pedestrian overtaking slower moving pedestrians has been observed, it has not been modeled. However, models for vehicle passing have been developed (e.g. [44]). We borrow from this model. Ahmed [44] found that lane changing depends on the difference between the speed that results from not changing lanes and the speed that could be achieved if the lane was changed. Specifically, a slightly simplified model for the probability of wanting to change lanes and overtake a slower node is

$$P(\text{desire to change lanes}) = 1/(1 + \exp(A + B(V_* - V^*))), \tag{2}$$

where V^* is the speed that the node would achieve if the nodes remains in the current lane and V_* is the speed that would be achieved if it changes lanes. Since speeds may experience short-term variation, instantaneous determinations of V^* and V_* leads to erratic behavior. Instead, letting v denote the node that is considering changing lanes, we define V^* to be the average speed of all nodes between v and the next intersection, and define V_* to be the minimum of the desired speed of v and the average speed of the nodes in the target lane that would be between v and the next intersection. Scaling the parameters found in [44], we set $A_{\text{Pedestrian}} = -0.225$, and $B_{\text{Pedestrian}} = 1.7$.

While this model has not been verified for pedestrians, in Section 6.3 we will see that it does give rise to realistic pedestrian clustering.

4.5. Mode of travel during commute

People may travel to and from work by car, by subway, and, for people who live within the simulated area, by walking. In the case of traveling to work by car, the trajectory of the person and the car matches until the car arrives at a parking lot to which the person is assigned (see Section 4.1). Once the person reaches the parking lot, they walk to their destination. Street parking is not considered here, but is considered by other traffic micro-simulators (e.g. [45]).

During subway travel, the person's trajectory starts at the subway stop and the person walks from the subway to their destination. We assume that subway trains arrive at Poisson distributed times, and hence people exit the subway in Poisson distributed bursts. As mentioned in [19], subway train arrivals can lead to platooning or clusters of pedestrians. Realistic mean time between subway arrivals is 3–10 min [46].

In American cities, the fraction of people who take mass transit widely varies, hence the UDel Models simulator allows this fraction to be adjusted. As points of reference, the national average of people who take mass transit to work in the US is 10.5% [47], but 87% of the people who enter Manhattan use mass transit [48].

4.6. Urban population size

It is well known that the number of users has a major impact on the performance of the network. Thus, realistic node population size is an important part of realistic simulation. While the number of nodes in a network depends on the number of people in the simulated region, it also depends on the fraction of people that subscribe to the network. Today, mobile phone penetration in Europe exceeds 80%, while in the US the fraction of subscribers is approximately 60%. Of course, in the early period of mobile phone deployment, the fraction of subscribers was much smaller. Hence, many penetration rates are realistic.

As expected, realistic populations size in an urban region can be quite large. For example, 1 km^2 of Manhattan may contain 10,000 people outdoors [19], a number that is far larger than most simulations currently found in the literature. However, if 10% of the population participates in the network, then a nine city-block region of Chicago would contain about 7000 nodes, a number that can be supported by protocol simulators such as QualNet [49]. The following presents guidelines for determining the population size in an urban region.

In the urban core, most of the indoor space is used for commercial purposes, including offices, stores, and restaurants, with office space being the most prevalent. A survey of office use in the UK found that typical densities are approximately 16.3 m^2 per person [50]. Thus, the total working population can be determined from the total area of office space.

The US Census American Housing Survey finds that in urban areas there is approximately 1 person per 65 m^2 of residential space. Thus, the size of the residential population can be computed from the total area of residential space. However, in the UDel Models it is assumed that 92% of the people that live in the city will also work within

the city, and hence are counted in the working population (the other 8% are not working).

The UDel Models sets the population as follows:

$$\text{Number of office workers} = \frac{\text{Total office area}}{15},$$

Number of people living within the city

$$= \min\left(\frac{\text{Total residential area}}{65}, \frac{\text{Number of office workers}}{0.92}\right),$$

Number of people in simulated region

$= \text{Number of office workers}$

$+ \text{Number of people living within the city}$

$\times 0.08 + \text{Number of nonworking visitors},$

Number of people who commute via subway

$= \text{MassTransitRatio} \times (\text{Number of office workers}$

$- \text{Number of people living within the city} \times 0.92),$

Number of people who commute via car

$= (1 - \text{MassTransitRatio}) \times (\text{Number of office workers}$

$- \text{Number of people living locally} \times 0.92),$

where the values are such that the office worker density is maintained even if there is an abundance of residential space. Note that we allow for some nonworking visitors. These people follow the same mobility as nonworkers that live within the city. However, further work is required to determine realistic sizes of the nonworking visitor populations. The MassTransitRatio is the fraction of commuters that take the subway, as discussed in Section 4.5.

5. Vehicle mobility

Vehicle mobility has been widely studied within urban planning and sophisticated simulators exist (e.g. [51–58]). However, these simulators often require more detailed information than is easily accessible to network researchers.

In general there are two types of vehicles, namely, commercial vehicles such as delivery vehicles and busses that make frequent stops, and private vehicles that make few stops. The UDel Models only considers private vehicles. For private vehicles, two types of trips are considered, trips where the car simply passes through the simulated region, and trips where the vehicle carries a person into or out of the simulated region. We first examine the case when the car simply passes through the simulated region.

Like the pedestrian model, a hierarchical model is used. However, only two tiers are used. The highest tier controls macro-mobility, i.e., it controls the flow of vehicles into the simulated region. The lower tier controls micro-mobility. The micro-mobility model is discussed next.

5.1. Micro-mobility

This lower tier is similar to the pedestrian mobility in that it includes the same structure for node interactions; specifically, the same framework for passing and speed–distance relationship is used. The distance–speed relationship is given by $D(S) = \alpha + \beta S$. For dry driving conditions, it

has been found that (α, β) ranges from $(1.45, 7.8)$ to $(1.78, 10.0)$ [59]. These values also agree with the observations presented in [60,61]. The probabilistic passing/lane changing model is discussed in Section 4.4.2, but the parameters in (2) are $A_{\text{Vehicle}} = -0.225$, $B_{\text{Vehicle}} = 0.1$. Unlike pedestrian traffic, vehicles never drive in the lanes used by the opposing traffic.

For vehicles, the ratio of the vehicle's desired speed to the speed limit presented in [62] can be modeled as Gaussian with mean 0.78 and standard deviation 0.26 (see Fig. 13).

5.2. Macro-mobility

Traffic engineering provides guidance on modeling the paths cars take through the modeled area. Traffic simulators such as VISSIM [54] allow vehicle trips to be generated in two ways, namely, with origin–destination (O–D) flow matrices or with turning probabilities. O–D matrices are much like the traffic matrix used in data network provisioning. The rate at which vehicles enter the simulated region at an origin O with desired destination D is given by the (O,D) element of the O–D matrix. If only turning probabilities are used, a vehicle enters into the modeled area at one of the pre-selected locations and proceed until the vehicle arrives at any exit location, which is at the edge of the modeled area or a parking location. At each intersection, vehicles turn or go straight according to the turning probabilities assigned to that intersection. O–D matrices yield a more accurate simulation, however, accurate O–D matrices are difficult to determine, whereas turning probabilities can be determined by simply counting vehicles turning at each intersection. Thus, both approaches are used for urban traffic engineering.

Drawbacks of turning probabilities are that vehicles might travel in long loops or meander through the city in unrealistic ways. However, since cars typically go straight (turning probabilities are typically between 0.1 and 0.3 [63,64]) such behavior is rare; most trips proceed through
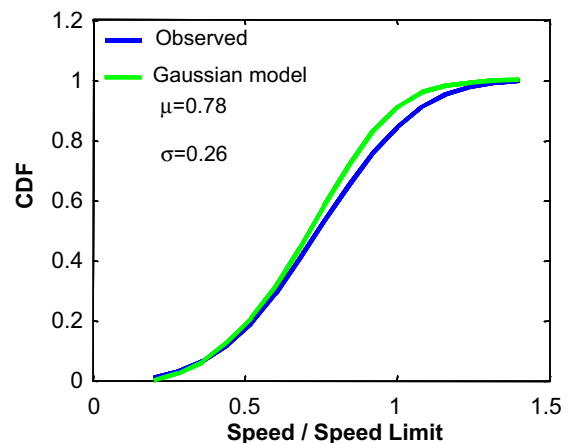

Fig. 13. The cumulative distribution Function (CDF) of the vehicle speed in urban areas and a fitted Gaussian CDF.

the city with only a few turns. The UDel Models currently uses homogeneous turning probabilities, i.e., the turning probability is the same at each intersection.

Each road that reaches the edge of the simulated area may have vehicles enter or exit at that point. Following the findings of [65], it can be assumed that vehicles enter the region as if they have just passed through a traffic light (i.e., in bursts), and that the number of vehicles in a burst is distributed according to a Poisson distribution. The mean number of vehicles per burst is not the same for each road. The distribution of flow rates for San Francisco streets is shown in Fig. 14 [66]. As is also shown in the figure, this distribution is well modeled by the mixture of two exponentials, specifically, P(Number of cars per day $> r$) = 0.74 $\exp(-r/8.9 \times 10^3) + (1 - 0.74)\exp(-r/1.3 \times 10^3)$. To convert the daily average flow shown in Fig. 14 to hourly flow, the scale factor from [67] shown in Fig. 15 is used. Thus, at the beginning of the simulation, a random number of total cars entering the simulated region are selected for each entrance point. Then, according to the simulated time, this random number is multiplied by a value shown in Fig. 15. The result is then divided by the length of the traffic light cycle (in hours). This value is used to determine the mean size of a burst of cars entering the through the entrance point.

While many vehicles may pass through the city, they may also carry people into or out of the city (we ignore the possibility that people use a car to travel within the city). In the UDel Models, when a person desires to exit the city via a car, they merely walk to their parking lot. Upon reaching the parking lot, the person enters a car and then proceeds to drive through the city until exiting the city. Similarly, when a person desires to enter the city, the next unoccupied car that enters the city is assigned to the person. This car proceeds to the desired parking lot assigned to the person. Upon arriving, the person exits the vehicle and walks to their office. While driving, the trajectory of the car is the same as the trajectory of the person.
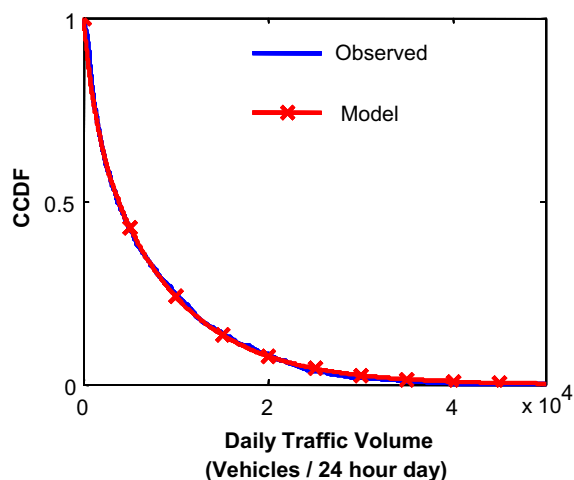

Fig. 14. The complementary cumulative distribution function of the vehicle traffic volumes on San Francisco streets.
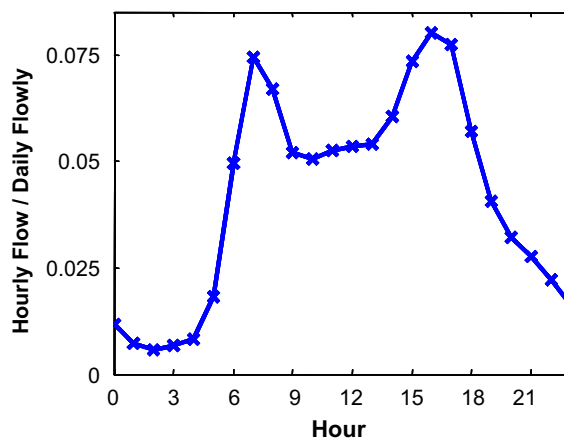

Fig. 15. The ratio of hourly volume to daily volume.

6. Model validation

The mobility model described in this paper is a combination of several components, with each component modeling a different aspect of mobility. While Sections 4 and 5 show that each component approximately models the data upon which the component is based, this section examines mobility metrics that are a result of several components of the model. Specifically, this section examines three mobility metrics. First, Section 6.1 examines the distribution of the duration of time that a pedestrians spends associated with an access point. The task and the activity models impact this duration. We compare this distribution to the distribution found from an actual wireless network. Second, we examine the number of pedestrians that walk down each sidewalk in a modeled region of Chicago. The agent and activity models as well as the population size model described in Section 4.6 impact this metric. This data is compared to actual pedestrian counts collected in Chicago. Third, we compare the pedestrian clustering that is generated by the agent model described in Section 4.4 to the clustering that was observed by [19]. The next three subsections will show that although the mobility model was not specifically designed to fit these metrics, the model provides a reasonably good fit.

6.1. The distribution of the time that a pedestrian is associated with an access point

In order to measure the distribution of the duration of time that a pedestrian is associated to an access point, we simulated a 9 city-block region of Chicago with the simulated start time of 6 a.m. and end time of 7 p.m. Using the UDel Models MapBuilder, we placed several access points on each floor of each building such that mobile nodes in any part of the building could communicate with at least one access point. We modeled the propagation with the UDel Models propagation tool. Mimicking 802.11 a/b/g, we assumed that a pedestrian could associate with an access point if the received signal strength from the access point exceeds −92 dBm when the transmission power is
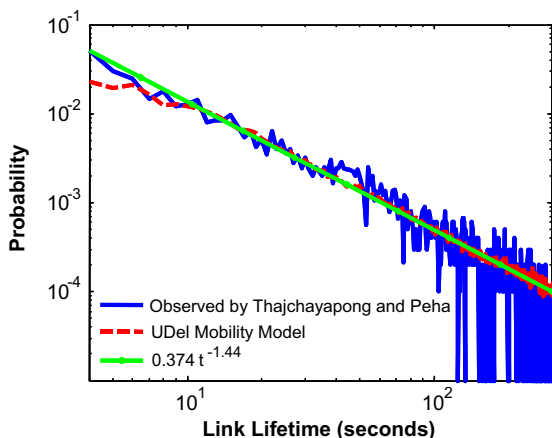
15 dBm. We further assumed that after a node becomes associated with an access point, it remains associated until the signal strength drops −92 dBm, at which point, it associates with the access point that has the strongest received signal strength. The duration that a pedestrian was associated with an access point, or *dwell time*, was recorded.

We compared the simulated dwell times with the dwell times collected by Thajchayapong and Peha [68] from a Carnegie Mellon University network. Their data was collected from July 1997 to December 1997. The network consisted of 90 access points in six buildings and had approximately 100 users. The dwell time for Thajchayapong and Peha study was defined in the same way as discussed above.

One of the main objectives of Thajchayapong and Peha's paper was to show that the dwell time in real networks has a heavy tail. More specifically, Thajchayapong and Peha found that the distribution of the dwell time is well modeled by a Pareto distribution with shape parameter of 1.44, which implies that the mean dwell time is finite and the variance of the dwell time is infinite. Fig. 16 is similar to Figs. 3a and 4 in [68]; it shows the PDF of the dwell time for dwell times greater than 4 s and the PDF of the Pareto distribution found by Thajchayapong and Peha, specifically, $p(t) = 0.374t^{-(1.44)}$. The empirical PDF found from the mobility model is also shown in Fig. 16. Observe that the tails of the three distributions are nearly the same. On the other hand, there is a lower quality of fit for dwell times less than 5 s. However, Thajchayapong and Peha indicated that these short dwell times are due to a node frequently switching between access points when signal strength from all access point is low. Thus, short dwell times are not caused by mobility of the node, but by the handoff protocol and by random variations in signal strength.

6.2. Validation of outdoor pedestrian density

The density of outdoor pedestrians depends on several components of the mobility model. Specifically, the activity model determines when pedestrians take trips outdoors and the distances traveled during the trip, and the agent model determines the speed at which the pedestrian travels. Together, these models determine the fraction of time that a person spends outdoors. The population model presented in Section 4.6 determines the number of people in the simulated area. Thus, the combination of these three models determines the number of outdoor pedestrians.

In order to determine the combined performance of these models, we simulated a region of Chicago with 9 city-block and 36 sidewalk segments, where a sidewalk segment is a one-block long sidewalk along one side of a street. The simulation started at a simulated time of 7:45 a.m. and ended at 5:45 p.m. The simulation modeled 21,012 people. We derived the map of the simulated region from GIS shape data, which includes the dimensions of the buildings in the region. Based on this data, we estimated that there is 1.04 km^2 of indoor area in this region. According to Section 4.6, such a region should have approximately 63,951 people, and hence the simulation simulated a factor of 3.04 less people than the estimated population. Using the resulting mobility trace data, we counted the number of pedestrians that walk on each sidewalk segment.

We compare the simulated pedestrian counts to those collected by the Chicago Loop Alliance (CLA), which has collected pedestrian counts for a 27 city-block region of downtown Chicago with 105 sidewalk segments [69]. Like the simulations described above, the CLA collected data from 7:45 a.m. to 5:45 p.m.

Table 4 shows the mean and standard deviation of the pedestrian counts over the 105 sidewalk measurements collected by the CLA. The table also shows 3.04 times the mean and standard deviation of the pedestrian counts over the 36 sidewalk segments from the simulation. The scaling factor is required since the number of pedestrians simulated is 3.04 times less than the estimated population of the simulated region. Observe that the mean pedestrian counts closely coincide, while standard deviations are slightly different. Nonetheless, we conclude that the pedestrian counts from the mobility model are realistic.

6.3. Validation of the agent model

Since the pioneering work of Pushkarev and Zupan [19], urban planners have known that pedestrians are not uniformly distributed but tend to be grouped into clusters or, in the terminology of urban planning, platoons. Platoons form for several reasons. For example, pedestrians form a cluster at a red traffic light that remains a cluster once the light turns green. Also, pedestrians exiting a subway train may form a platoon [19]. The agent model described in Section 4.4 also impacts platooning. Specifically, the

Fig. 16. PDF of the dwell time as found by Thajchayapong and Peha [68], the PDF of the dwell time from the UDel Mobility Model, and the PDF of a Pareto random variable that Thajchayapong and Peha found as a model of the dwell time.

Table 4
Statistics of pedestrian counts in downtown Chicago

	Observation by the CLA	Mobility model $\times$ 3.04
Mean pedestrian count	1.065×10^4	1.089×10^4
Standard deviation	4.61×10^3	7.07×10^3
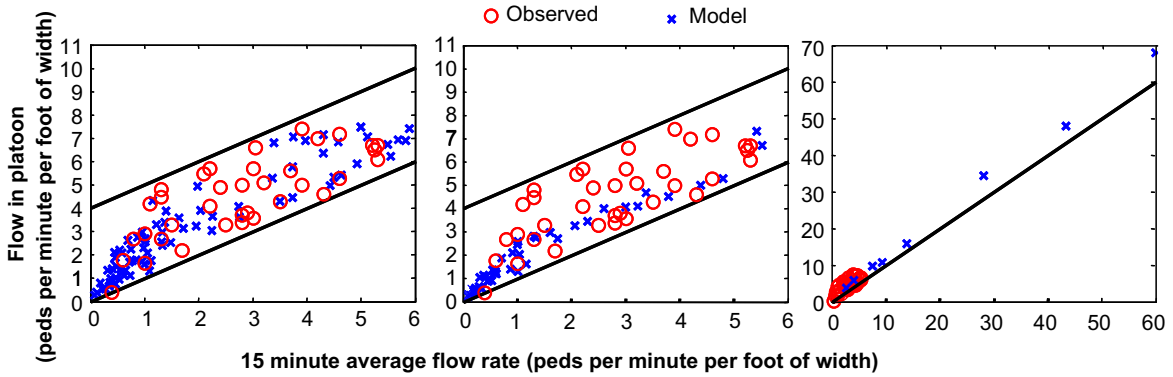
Fig. 17. A validation of the pedestrian agent model. The black lines are the ranges that Pushkarev and Zupan considered realistic. The circles are values that Pushkarev and Zupan observed and the x-marks are the values generated by the simulator. The left-hand frame shows the results of the full simulator. The middle frame shows the results when no probabilistic passing model is used; instead a node always passes. The right-hand plot is when no inter-node dynamics are used, e.g., two nodes can occupy the same location.

passing model dictates that when a faster moving nodes catches up to a slower moving node, it does not necessarily pass, but instead follows the node resulting in a cluster or growing an existing cluster.

Platoons are important in wireless networks. Specifically, nodes in a cluster will experience strong interference from transmissions by other nodes in the cluster. Hence, platooning will act to increase the interference that nodes experience as compared to the case when nodes are uniformly distributed. On the other hand, the mobility model described in this paper does not directly model platooning. Instead, platooning is a by-product of the agent model described in Section 4.4, traffic lights, and, to some extent, subways. In order to validate platooning generated by the model described in this paper, we use the observations made by Pushkarev and Zupan [19].

While Pushkarev and Zupan's work has served as the basis for the pedestrian traffic engineering guidelines set forth in the Highway Capacity Manual [20], the metrics of burstiness used are different from the ones typically used in studying burstiness in data networks. Specifically, Pushkarev and Zupan compare two flow metrics, the 15-min average flow rate (AFR) and the flow rate during a platoon (PFR). A node is declared to be in a platoon if the local density of nodes exceeds the average density. As is shown in Fig. 17, the PFR is higher than the AFR. According to Pushkarev and Zupan, the larger the PFR is as compared to the AFR, the more bursty the pedestrian traffic. The study of Pushkarev and Zupan was not focused on finding the frequency of specific flow rates, but to examine what combinations of AFR and PFR occur on urban sidewalks. Thus, we use this data as a baseline with which we compare the pedestrian mobility model described above.

The left-hand plot in Fig. 17 shows two sets of data. The generated data from the mobility model is from a variety of configurations including counting pedestrians on a block with and without buildings, various sizes of sidewalks (from 4 lanes to 32 lanes), various traffic light timings (from 60 s to 120 s periods), and various rates of pedestrians flowing into the street. As can be seen from the left-hand plot in Fig. 17, the mobility model described above generates combinations of PFR and AFR that are realistic.

The center plot in Fig. 17 shows the data set collected by Pushkarev and Zupan and a set of data generated by the mobility model but where nodes pass whenever there is room to pass, i.e., P(desire to change lanes) ≡ 1 as oppose to what is given in (2). Clearly, increasing the propensity to change lanes acts to decrease the burstiness so that some realistic levels of burstiness never occur. Finally, the right-hand plot in Fig. 17 shows Pushkarev and Zupan's data compare to data generated by the mobility model but where there are no inter-pedestrian dynamics, i.e., nodes move along lanes irrespective of other nodes. Such mobility allows, for example, nodes to disobey the distance–speed relationship. As shown in Fig. 17, ignoring inter-node dynamics results in unrealistic levels of congestion (extreme discomfort occurs when the flow rate exceeds 7 [19]).

7. Impact of mobility on network performance

This section investigates the impact of realistic mobility on simulated network performance. A general investigation of network performance and mobility models is difficult since the impact on the network performance depends on the specific metric and/or protocol(s) of interest. Furthermore, there are a large number of types of mobility (e.g., indoor, outdoor, pedestrian, and vehicle), and, as described above, there are many aspects of mobility (e.g., speed and node interaction). Thus, only of some of the impacts that realistic mobility has on performance are examined.

In the analysis that follows, the realistic mobility is generated by the UDel Models version 2.0 [22]. We based these simulations on a 3×3 block region of downtown Chicago with 54 fixed wireless relays placed on lampposts that are uniformly distributed throughout the region. We used the UDel Models to generate realistic propagation for this region [18]. In several experiments below, CBR traffic is sent from a base station to a mobile node, where the base station was located in the northwest corner of the simulated region. The CBR traffic consisted of 100B packets every 500 ms. 802.11b at 2 Mbps was used for all transmissions with RTS/CTS enabled. AODV routing was used [70].

7.1. Trip types

Urban mobility includes a diverse set of types of trips. In order to explore the impact of the trip type on network performance, seven types of trips were defined (see Fig. 18). For each trip type, a mobility trace for the time period 2:45 p.m. to 3:15 p.m. was searched for the desired type of trip. An application configuration file was generated so that CBR traffic was sent from the base station to the mobile node during the desired trip. There was only one flow for each simulation trial. The simulations each ran for 100 s, except, for simulations of indoors to outdoors to indoors trips, which started as the node began to move and ended when it stopped moving. It was ensured that such trips lasted at least 100 s. Fig. 18 shows the loss probability for the different trip types averaged over 10 trials. Clearly, the trip type has a significant impact on the performance. While the quantitative impact of the trip type could not be predicted, as explained next, the qualitative impact is expected.

Since nodes on the lower floors are within the communication range of the infrastructure nodes, routes from the base station to nodes on the lower floors are likely to be composed of infrastructure nodes. Consequently, connections to stationary nodes on the lower floors (trip type 1) have low loss probability. sAs a result of paths failures due to the mobility, connections to nodes moving on the lower floors (trip type 3) suffer more losses than stationary nodes on the lower floors. However, since these nodes remain within the communication range of the infrastructure, the loss probability remains low. In contrast, paths to stationary nodes on the upper floors must include *mobile* nodes on other floors. Hence, connections to stationary nodes on upper floors (trip type 2) suffer more losses than connections to nodes on the lower floors. And when the nodes on the upper floors move, the loss probability is further increased.

Wireless signals propagate much further outdoors than indoors. Thus, connections to outdoor pedestrians (trip type 6) have few path failures and hence experience low loss probability. Due to the higher rate of mobility, connections to vehicles (trip type 7) have a slightly higher loss probability. Note that outdoor pedestrians and vehicles have paths of the same length, but due to the higher speed

of vehicles, the probability of packet loss to vehicle is higher than it is for outdoor predestrians. Finally, connections to nodes that move from indoors to outdoors and back indoors (trip type 5) experience a fairly high loss probability. This behavior is due to the path failures that occur when the node moves from indoors to outdoors and back indoors and when the node is changing floors. Note, that trip type 4 does not distinguish between whether the node's starting or ending point was on the upper or lower floors. Comparing the number of hops for trip types 3 and 5 and the probability of packet loss for these trip types, we see that the number of hops is not necessarily a good predictor of the packet loss; the mobility is also important.

7.2. Random office waypoint

Random waypoint is a popular mobility model for exploring the performance of MANETs. Random office waypoint (ROW) is an urbanized extension of random waypoint. In this model, a pedestrian walks to an office randomly selected from any building. Upon reaching the office, the pedestrian pauses for an exponentially distributed amount of time, and then selects a new office and repeats the process. The office pause times are set to 19 min, matching the office pause times of the UDel Mobility Model. ROW is slightly different from City Section mobility model [71], which considers streets and roads, not offices in a building as a destination. In the next three subsections, the ROW model is compared to realistic mobility.

7.2.1. Trip types

In order to compare the impact that the ROW model and realistic mobility model have on performance, the destination of a test connection was selected in three ways. In the first case, the destination was selected so that when the simulation began, the node was stationary and indoors. In the second case, the destination was selected so that when the simulation began, the mobile node had just begun to move. And in the third case, the destination was selected at random regardless of whether the node is moving. In all cases, the simulation ran for 300 s. Section 7.1 showed that the floor that a node is on has a significant impact on the packet loss probability. Thus, in order to focus on the impact of mobility and not be distracted by the

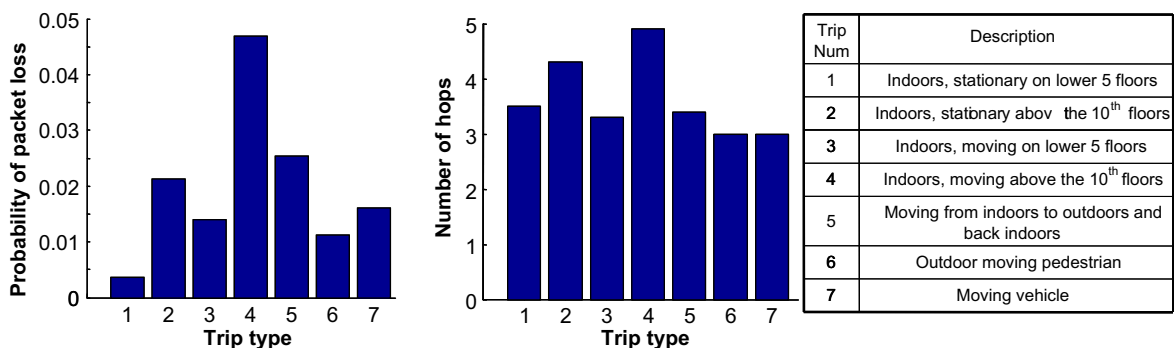| Trip Num	Description
1	Indoors, stationary on lower 5 floors
2	Indoors, stationary abov the 10th floors
3	Indoors, moving on lower 5 floors
4	Indoors, moving above the 10th floors
5	Moving from indoors to outdoors and back indoors
6	Outdoor moving pedestrian
7	Moving vehicle

Fig. 18. Loss probability and number of hops for different types of trips.

floor that nodes are on, in this section, all nodes were restricted to the lower five floors of buildings.

The main difference between ROW and realistic mobility is that in ROW, nodes tend to take long outdoor trips, whereas in realistic urban mobility, most mobile trips are short and do not include an outdoor component. As a result, in ROW, nodes tend to spend more time moving and much of this time is outdoors. As explained next, the impact of these differences are detectable in packet loss probability shown in Fig. 19.

Since nodes often take long outdoor trips in the ROW model, there are more mobile nodes outdoors under the ROW model than under realistic mobility. Consequently, under the ROW model, a route found by AODV from an outdoor base station is more likely to include outdoor mobile nodes than it is under realistic mobility, in which case the route is more likely to use the lamppost-mounted relays. As a result, connections to stationary nodes have a higher loss probability under the ROW model than under realistic mobility.

In the mobile case, under the ROW model, nodes tend to take indoor–outdoor–indoor trips (since a randomly selected next office is typically in a different building), whereas in the mobility models presented in this paper, a typical trip remains indoors. As shown in Fig. 18, indoor–outdoor–indoor trips suffer a higher loss probability than indoor trips. Moreover, under realistic mobility, nodes take short trips, and hence spend much of their time not moving. Thus, when a node is selected at random, the probability of packet loss for realistic mobility is similar to the probability of packet loss of stationary nodes. On the other hand, under the ROW model, nodes spend a larger fraction of time moving. Thus, when a node is selected at random, the probability of packet loss is approximately half way between the value obtained when the nodes are stationary and the value obtained when the nodes are mobile.

7.2.2. Node clustering

As mentioned in Section 4.4 and 6.3, node interactions lead to node clustering. One result of node clustering is that nodes will have a larger number of nearby neighbors
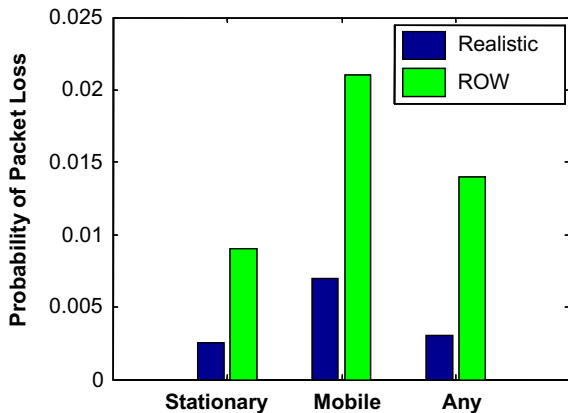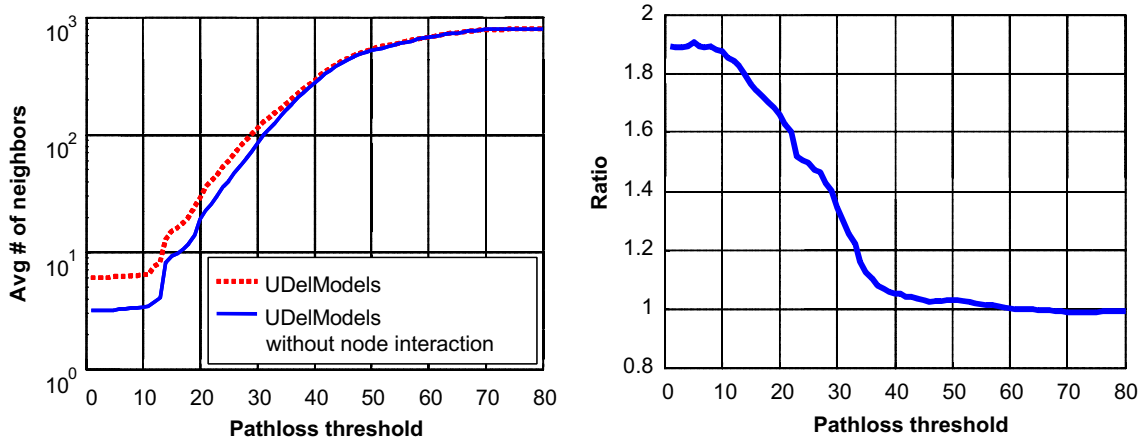
than they would if nodes were more uniformly spread. Fig. 20 demonstrates this effect by showing the average number of neighbors as a function of the channel loss. Specifically, let $N_i(H)$ be the number of nodes j such that the channel loss between node i and j is at least as strong as H. The left-hand side of Fig. 20 shows the average value of $N_i(H)$, averaged over all outdoor nodes i. This figure shows the average when node interaction is enabled and when it is disabled. The right-hand side of Fig. 20 shows the ratio of the average value of $N_i(H)$ when node interaction is enabled and the average value of $N_i(H)$ when node interaction is disabled. Since the channel to nearby nodes have low channel loss, clustering results in an increase in the number of nodes with low channel loss. For example, the average number of nodes with a channel loss lower than 10 dB is increased by nearly a factor of two. However, clustering does not greatly impact the number of nodes that are at greater distances (e.g., with channel loss of 60 dB). Of course, the impact that clustering has on network performance depends on the metric and protocol. For example, clustering will increase interference with nearby nodes. However, with such good channels, very high data rate communication to nearby nodes is possible. This property could be used to construct ad hoc virtual antennas.

### 7.2.3. Mobility management – the number of infrastructure nodes seen

Large-scale mesh networks are expected to have thousands of mobile users. Advanced mobility management schemes are necessary to support user mobility in a scalable fashion. In order to determine the performance of such mobility management schemes, realistic mobility is required. For example, if users are only able to communicate with a small number of infrastructure nodes (INs) through the course of a typical day, it is feasible for the INs to maintain per user profiles. However, such an approach would not be feasible if users typically visit a large number of INs. Fig. 21 shows the average of the cumulative number of INs that a user hears throughout the day for UDel Models and the ROW model. In the case of the UDel Models, the beginning of the day is marked by a rapid increase in the cumulative number of infrastructure nodes heard. However, once most people arrive at work (around 9 a.m.), the rate that new INs are heard decreases. Since people may explore new areas of the city during a lunchtime trip, the number of new INs heard slightly increases around noon. On the other hand, under the ROW model, nodes continually explore large regions of the city. Hence, a large number of INs are heard and the number heard continually increasing throughout the day. Thus, maintaining per user profiles appears considerable more difficult under the ROW model than under the mobility models presented in this paper.

7.3. Node interaction in vehicle networks

The dynamics of car mobility include passing, queuing at traffic lights, and obeying traffic lights. Without these dynamics, cars move at a constant speed while occasionally making turns. Such a model is similar to the Manhattan Mobility Model [72]. In order to investigate the

Fig. 19. Packet loss probability for random office waypoint (ROW) and realistic mobility for different types of trips.

Fig. 20. Impact of clustering. Clustering results in nodes having a larger number of neighbors with low channel loss than if the nodes are not clustered. As shown, clustering increases number of neighbors with low channel loss.
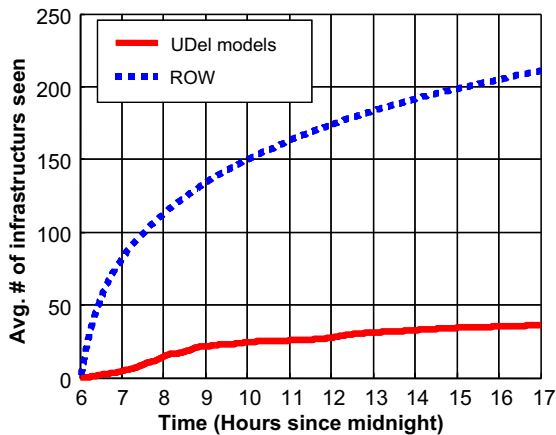
Fig. 21. Average cumulative number of infrastructure nodes heard by a mobile node throughout the day for the Random Office Waypoint (ROW) mobility model and the UDelModels mobility model.

impact of the vehicle mobility model, the CBR data traffic was sent from a base station to a randomly selected car. The cars were selected at random under the constraint that the car remained in the simulated region for at least 100 s, which was the connection duration. The simulated time was 5:30 p.m. It was found that the full mobility model resulted in a loss probability of 0.016, whereas when the dynamics of vehicle mobility was neglected, the loss probability jumped to 0.064, an increase by a factor of four. Recall that TCP provides very low throughput when the loss probability exceeds 5% [73]. Thus, the realistic mobility results in the conclusion that TCP will perform reasonably well, whereas, the unrealistic model leads to the opposite conclusion.

8. Related work

As [31,74] categorized, UDel mobility model is the first survey-based mobility model [75]. In terms of macro-

mobility methodology, the mobility models that are most similar to the model presented here are [76–78]. In [76], the authors used US National Household Travel Survey data to obtain various distributions, including activities, occupations and dwell times. However, their model only considers outdoor locations, and pedestrians are constrained to a 2-D grid. Hence, this model is similar to the City Section Mobility Model described in Section 7.2, but instead of selecting destinations and pause duration randomly, [76] uses data from the US National Household Travel Survey.

GEMM [77] is an agent-based model where several factors impact the mobility of the node. For example, GEMM includes attraction points as well as habits to influence the mobility. A noted drawback of this work is that realistic values of the model parameters are unknown.

The model presented in [78], known as CanuMobiSim, shares several features with the UDel mobility model. For example, both models allow real maps to be used and have pedestrian and vehicle mobility models. However, Canu-MobiSim lacks indoor mobility. Moreover, CanuMobiSim assumes that pedestrians move from location to location according to a Markov chain where each location has a pre-defined type (e.g., restaurant). The locations can be points of interests that are defined by the map or defined by the user. However, like [77], it is unclear how to define the parameters of the Markov chain so that the resulting mobility is realistic. VanetMobiSim [79] extends CanuMo-biSim to include traffic lights, stop signs, and passing models. The UDel Models also includes traffic lights and passing models, but does not include stop signs.

As defined in [31], other mobility models can be roughly divided into three classes, namely synthetic models, trace-based mobility models, and mobility models from urban planning. While [31] provides a detailed review of these classes of models, a brief review is as follows.

Synthetic models are perhaps the most well known class of mobility models. A simple probabilistic model characterizes these models. Representative models in this class are Random Walk [80], Random Waypoint [81],

Random Direction [82], Reference Point Group Mobility Model [83], City Section Model [71], and Manhattan Model [14]. While the Manhattan Mobility Model used idealized grid-cities, several researchers have used actual city maps from the TIGER data sets [26] (e.g. [27,29,28]), whereas [84] uses a random graph. In many of these graph-constrained cases, the mobility is essentially random waypoint, but restricted to a graph. [85] is another example of constrained random waypoint, but where the graph and mobility parameters depend on the scenario under consideration. [86,87] revealed various flaws and limitations of simple models based on some form of random walk or waypoint. Moreover, [88] noted that most of the models are not realistic enough for network protocol performance evaluation.

The second class is trace-based mobility models. Unlike synthetic models, models in this class are extracted from real world traces such as handoff and association in LANs. For example, [89–91] extracted mobility models from campus-wide networks. Tuduce [89] showed that WLAN mobility model yields lower mobility characteristics than the synthetic mobility models. However, the data used in this study did not differentiate between laptops and more mobile terminals such as PDAs. In fact, McNett and Voelker [90] analyzed the mobility patterns of users of wireless handheld PDAs and found that the PDA users were about twice as mobile as laptop. Kim and Kotz [91] generated a random waypoint model with speed and pause time distributions from traces from wireless VoIP users. Other traced-based mobility models include [92,93], which focus on models based on observations of pedestrians on a university campus.

Maeda et al. [94] presents a type of trace-based urban mobility model. This algorithm takes as input the flow edge rates of a simulated area, i.e., the rate that pedestrians enter or exit the simulated region at each walkway that crosses the edge of the simulated region. From these values, mobility within the simulated region is estimated. Since this scheme uses actual mobility measurements, it is inherently realistic. However, the derived mobility model is specific to the region where the measurements are performed. Maeda et al. [94] did not investigate how to extend the specific mobility model generated to a more general one that can be applied in other scenarios (e.g., other maps).

The third class of mobility models are those whose original purpose was for urban planning. Simulators that belong to this class include VISSIM [51], SUMO [52], CARISMA [53], CORSIM [54], Paramics [55], TRANSIMS [56], and MMTS [57,58]. The main drawbacks of these simulators are that they complicated to use and not directly suitable for wireless network simulation. Moreover, several of these simulators are expensive and/or only simulate vehicles. There have been efforts focused on developing tools so that these simulators can be used for network simulation. For example, Karnadi et al. [95], Piorkowski et al. [96] developed tools for SUMO, Baumann and Heimlicher [97] developed tools for MMTS, Eichler et al. [98] developed tools for CARISMA, a proprietary simulator used by BMW, and Lochert et al. [99] developed tools for VISSM, a commercial simulator. In all of these cases, the focus has been on vehicle networks.

9. Future work in mobility

There are several areas of realistic urban mobility simulation that require further effort. One important area is mobility during disasters, crisis, and other events (e.g., Independence Day celebrations). Disasters and crisis mobility requires mobility models not only of the civilians, but also of emergency personnel. Note that both Philadelphia and San Francisco specify that their mesh network will be used to enhance emergency communication. Also, the discussion above and the current version of the UDel Models only consider cars. However, buses and commercial trucks should also be considered. For example, network protocols for such commercial vehicles are already under development (e.g. [100–102]).

The mobility models developed above are mostly derived from statistics collected in the US. However, use of time and the agent models of both vehicles and people depend on the country. Much of the data used here is also available for other countries. Hence, future work will develop mobility models for cities in other countries besides the US. Similarly, the focus of the model is mostly on office workers and nonworkers, the dynamics of nonoffice workers still needs to be explored and incorporated into the simulator.

Group mobility is a popular class of mobility models. However, there has been little work on realistic group mobility. One situation where group mobility commonly occurs in the urban setting is when groups of office workers go to lunch. An informal study performed in Philadelphia found that the number of people in a group followed the Zipf distribution with shape parameter of 2.18, i.e., P(Group size $\geqslant g$) = $1/g^{2.18}$. However, further study of group sizes and group mobility dynamics is required.

10. Conclusions

A methodology for realistic simulation of urban mobility was presented. The techniques described have been implemented in a suite of simulation tools that are available for download [22]. The techniques presented are based on data collected from a wide range of sources. For example, the activities that people perform are derived from the 2004 US Bureau of Labor Statistics survey on time use. The detailed mobility model of people and vehicles is derived from modeling methodologies and data collected by the urban and traffic planning community. Vehicle traffic flows are derived from data collected by the City of San Francisco and the State of Connecticut. The density of people is derived from surveys of office space use and the US Census American Housing Survey. Other aspects of the model are derived from other data. In all, much of the model is based on surveys and observations of the mobility of people and vehicles.

While the mobility model presented here is considerably more realistic than models often used in mobility wireless networking research, realistic mobility alone will not produce realistic simulations. Along with realistic protocol and physical layer simulation, it is critical to model the channel realistically. Therefore, the techniques discussed here are incorporated into a simulation package such as [22] that includes propagation simulation.

Disclaimer

The views and conclusions contained in this document are those of the authors and should not be interpreted as representing the official policies, either expressed or implied, of the Army Research Laboratory or the U.S. Government.

References

[1] K. Dell, Welcome to wi-fi-ville, Time Magazine.
[2] The City of Corpus Christi, Corpus Christi WiFi, 2007.
[3] H. Xie, S. Tabbane, D. Goodman, Dynamic location area management and performance analysis, in: Proceedings of 43rd IEEE Vehicular Technology Conference, 1993, pp. 535–539.
[4] J. Markoulidakis, G. Lyberopoulos, D. Tsirkas, E. Sykas, Evaluation of location area planning scenarios in future mobile telecommunication systems, Wireless Networks 1 (1) (1995) 17–29.
[5] S.J. Kim, C.Y. Lee, Modeling and analysis of the dynamic location registration and paging in microcellular systems, IEEE Transactions on Vehicular Technology 45 (1) (1996) 82–90.
[6] A. Hac, Z. Zhou, Locating strategies for personal communication networks: a novel tracking strategy, IEEE Journal on Selected Areas in Communication 15 (8) (1997) 1425–1436.
[7] A. Bar-Noy, I. Kessler, Tracking mobile users in wireless networks, IEEE Transactions on Information Theory 39 (1993) 1877–1886.
[8] S. Bohacek, V. Sridhara, L. Lou, Efficient paging in large-scale urban mesh networks, in: Proceedings of the 4th International Workshop on Wireless Mobile Applications and Services on WLAN Hotspots, ACM, 2006. pp. 81–90.
[9] W. Ren, D.-Y. Yeung, H. Jin, TCP performance evaluation over AODV and DSDV in RW and SN mobility models, Journal of Zhejiang University – Science A 7 (2006) 1683–1689.
[10] G. Holland, N. Vaidya, Analysis of TCP performance over mobile ad hoc networks, Wireless Networks 8 (2002) 275–288.
[11] B. Divecha, A. Abraham, C. Grosan, S. Sanyal, Analysis of dynamic source routing and destination-sequenced distance-vector protocols for different mobility models, in: Proceedings of the First Asia International Conference on Modelling and Simulation (AMS'07), 2007.
[12] B.-R. Chen, C.H. Chang, Mobility impact on energy conservation of ad hoc routing protocols, in: International Conference on Advances in Infrastructure for Electronic Business, Education, Science, Medicine, and Mobile Technologies on the Internet SSGRR 2003, 2003.
[13] X. Hong, T.J. Kwon, M. Gerla, D.L. Gu, G. Pei, A mobility framework for ad hoc wireless networks, in: Proceedings of ACM Second International Conference on Mobile Data Management (MDM'01), 2001.
[14] F. Bai, N. Sadagopan, A. Helmy, The important framework for analyzing the impact of mobility on performance of routing protocols for ad hoc networks, Ad Hoc Networks 1 (2003) 383–403.
[15] P. Prabhakaran, R. Sankar, Impact of realistic mobility models on wireless networks performance, in: IEEE International Conference on Wireless and Mobile Computing, Networking and Communications (WiMob), 2006, pp. 329–334.
[16] M. Bhatt, R. Chokshi, S. Desai, S. Panichpapiboon, N. Wisitpongphan, O.K. Tonguz, Impact of mobility on the performance of ad hoc wireless networks, in: 2003 IEEE 58th Vehicular Technology Conference, 2003.
[17] T. Rappaport, Wireless Communications – Principles and Practice, Prentice Hall, 2002.
[18] V. Sridhara, S. Bohacek, Realistic propagation simulation of urban mesh networks, Computer Networks: The International Journal of Computer and Telecommunications Networking 7 (2006) 1683–1689. <http://udelmodels.eecis.udel.edu>.
[19] B. Pushkarev, J.M. Zupan, Urban Space for Pedestrians, MIT press, 1975.
[20] Transportation Research Board, 2000 Highway Capacity Manual, National Research Council, Washington, DC, 2000.
[21] A. Szalai, The Use of Time, Mouton, The Hague, 1972.
[22] S. Bohacek, V. Sridhara, J. Kim, UDel models for simulating urban wireless networks. <http://udelmodels.eecis.udel.edu/>.
[23] A. Jardosh, E.M. Belding-Royer, K.C. Almeroth, S. Suri, Towards realistic mobility models for mobile ad hoc networks, in: MobiCom, 2003.
[24] S. Bohacek, V. Sridhara, The graphical properties of MANETs in urban environments, in: The Forty-Second Annual Allerton Conference on Communication Control and Computing, 2004.
[25] Geographic information system (GIS). <http://www.gis.com>.
[26] US Census Bureau, Topologically integrated geographic encoding and referencing (TIGER). <http://www.census.gov/geo/www/tiger/>.
[27] R. Mangharam, D.S. Weller, D.D. Stancil, R. Rajkumar, J.S. Parikh, GrooveSim: a topography-accurate simulator for geographic routing in vehicular networks, in: Proceedings of the 2nd ACM International Workshop on Vehicular Ad Hoc Networks, ACM, Cologne, Germany, 2005. pp. 59–68.
[28] A.K. Saha, D.B. Johnson, Modeling mobility for vehicular ad hoc networks, in: Proceedings of the 1st ACM International Workshop on Vehicular Ad Hoc Networks, ACM, Philadelphia, PA, 2004. pp. 91–92.
[29] D.R. Choffnes, F.E. Bustamante, An integrated mobility and traffic model for vehicular wireless networks, in: Proceedings of the 2nd ACM International Workshop on Vehicular Ad Hoc Networks, ACM, Cologne, Germany, 2005. pp. 69–78.
[30] N.C. Romano, J.F. Numamaker, Meeting analysis: findings from research and practice, in: Proceedings of Teh 34th Hawaii International Conference on Systems Science, 2001.
[31] J. Haerri, F. Filali, C. Bonnet., Mobility models for vehicular ad hoc networks: a survey and taxonomy, Tech. Rep., EURECOM, 2007.
[32] US Department of Labor Bureau of Labor Statistics, American Time Use Survey (ATUS), 2003. <http://www.bls.gov/tus/>.
[33] V. Sridhara, J. Kim, S. Bohacek, Performance of urban mesh networks, in: The 8th ACM/IEEE International Symposium on Modeling, Analysis and Simulation of Wireless and Mobile Systems, 2005.
[34] R.R. Panko, S.T. Kinney, Meeting profiles: size, duration, and location, in: Proceedings of the 28th Annual Hawaii International Conference on Systems Science, 1995.
[35] R.K. Mosvick, R.B. Nelson, We've Got to Start Meetings Like This!, Scott, Foresman and Company, Glenview, Illinois, 1987.
[36] Feller, An Introduction to Probability Theory and Its Applications, Wiley, 1968.
[37] S.J. Older, Movement of pedestrian on footways in shopping street, Traffic Engineering and Control (1968) 160–163.
[38] F.P.D. Navin, R.J. Wheeler, Pedestrian flow characteristics, Traffic Engineering (1969) 30–36.
[39] D. Oeding, Traffic loads and dimensions of walkways and other pedestrian circulation facilities, Strassenbau and strassenverkehrs-technik 22 (1963) 160–163.
[40] D. Helbing, Sexual differences in human crowd motion, Nature 240 (1972) 252.
[41] D. Helbing, The statistics of crowd fluids, Nature 229 (1971) 381.
[42] G.K. Still, Crowd dynamics, Ph.D. Thesis, University of Warwick, 2000.
[43] Y. Zhang, L.E. Owen, J.E. Clark, A multi-regime approach for microscopic traffic simulation, in: The 77th TRB Annual Meeting, 1998.
[44] K.I. Ahmed, Modeling drivers' acceleration and lane changing behavior, Ph.D. Thesis, MIT, 1999.
[45] V. Mauro, Evaluation of dynamic network control: simulation results using NEMIS urban micro-simulator, in: Transportation Research Board Annual Meeting, Washington DC, 1991.
[46] Massachusetts Bay Transportation Authority. <http://www.mbta.com>.
[47] <http://www.transact.org/report.asp?id=190>.
[48] <http://www.transalt.org/info/SOVBanImpacts.pdf>.
[49] QualNet Network Simulator. <http://www.scalable-networks.com/>.
[50] M. Wist, Office space – how much is enough? Tech. Rep., Gerald Eve, 2001.
[51] PTV Simulation VISSIM. <http://www.english.ptv.de/>.
[52] SUMO Simulation of Urban MObility. <http://sumo.sourceforge.net/>.
[53] S. Eichler, B. Ostermaier, C. Schroth, T. Kosch, Simulation of car-to-car messaging: analyzing the impact on road traffic, in: MASCOTS'05, 2005.
[54] FHWA, CORSIM User's Manual, Version 5.0, ITS Research Division, FHWA, 2000.
[55] Paramics. <http://www.paramics-online.com/>.
[56] TRANSIMS. <http://transims.tsasa.lanl.gov/>.
[57] B. Raney, A. Voellmy, N. Cetin, M. Vrtic, K. Nagel, Towards a microscopic traffic simulation of all of Switzerland, in: ICCS'02, 2002.

[58] B. Raney, N. Cetin, A. Vollmy, An agent-based microsimulation model of swiss travel: first result, Networks and Spatial Economics 3 (2004) 23–41.

[59] S. Shekleton, A GPS study of car following theory, in: Conference of Australian Institutes of Transport Research (CAITR), 2002.

[60] T. Dijker, P.H.L. Bovy, R.G.M.M. Vermijs, Car following behavior in different flow regimes, in: P.H.L. Bovy (Ed.), Motorway Traffic Flow Analysis, Delft University Press Delft, The Netherlands, 1998, pp. 49–70.

[61] J. Piao, M. McDonald Analysis of stop and go driving behavior through a floating vehicle approach, in: Proceedings of the IEEE Inteligent Vehicles Symposium, 2003.

[62] J. Du, L. Aultman-Hall, An investigation of the distribution of driving speeds using in-vehicle GPS data, in: Vermont Institute of Transportation Engineers Annual Meeting, 2004. <http://www.neite.org/vt/dist12004/>.

[63] J.E. Hummer, Unconventional left-turn alternatives for urban and suburban arterials, ITE Journal 68 (1998) 101–106.

[64] M.J. Bayarri, J.O. Berger, G. Molina, N.M. Rouphail, J. Sacks, Assessing uncertainties in traffic simulation: a key component in model calibration and validation, Tech. Rep. 137, National Institute of Statistical Sciences, 2003.

[65] A. Kamarajugadda, B. Park, Stochastic traffic signal timing optimization, Tech. Rep. UVACTS-15-0-44, Center for Transportation Studies at the University of Virginia, 2003.

[66] City of San Francisco Department of Parking and Traffic, Daily Traffic Volume. <http://www.sfgov.org/site/uploadedfiles/dpt/Volumes% 20Web.pdf>.

[67] J.N. Ivan, W. ElDessouki, M. Zhao, F. Guo, Estimating link traffic volumes by month, day of the week, and time of day, Tech. Rep. JHR 02-287, Joint Highway Research Advisory Council of the University of Connecticut, 2002.

[68] S. Thajchayapong, J.M. Peha, Mobility patterns in microcellular wireless networks, IEEE Transactions on Mobile Computing 5 (2006) 20–27.

[69] Chicago Loop Alliance, Pedestrian Traffic Counts. <http://www.chicagoloopalliance.com/businessintheloop/economicstudy/pedestrian.htm>.

[70] C.E. Perkins, E.M. Royer, Ad hoc on-demand distance vector routing, in: Proceedings of the 2nd IEEE Workshop on Mobile Computing Systems and Applications, 1999, pp. 90–100.

[71] V. Davies, Evaluating mobility models within an ad hoc network, Master's Thesis, Colorado School of Mines, 2000.

[72] F. Bai, N. Sadagopan, A. Helmy, Important: a framework to systematically analyze the impact of mobility on performance of routing protocols for ad hoc networks, in: InfoCom, 2003.

[73] S. Bohacek, K. Shah, A model of TCP's throughput and time-out probablity – steady-state and time-varying dynamics, in: GlobeCom, 2004.

[74] P. Sommer, Design and analysis of realistic mobility model for wireless mesh networks, Master's Thesis, ETH Zurich, 2007.

[75] J. Kim, S. Bohacek, A survey-based mobility model of people for simulation of urban mesh networks, in: The First International Workshop on Wireless Mesh Networks (MeshNets'05), 2005.

[76] Q. Zheng, X. Hong, J. Liu, An agenda based mobility model, in: Proceedings of the 39th Annual Simulation Symposium (ANSS'06), 2006.

[77] S. Ray, Realistic mobility for MANET simulation, Master's Thesis, The University of British Columbia, 2003.

[78] I. Stepanov, P. Marron, K. Rothermel, Mobility modeling of outdoor scenarios for MANETs, in: Proceedings of 38th Annual Simulation Symposium (ANSS'05), 2005.

[79] J. Haerri, F. Filali, C. Bonnet, M. Fiore, VanetMobiSim: generating realistic mobility patterns for VANETs, in: VANET'06, 2006.

[80] A. Einstein, Investigations on the theory of the Brownian motion, Dover, New York.

[81] D. Johnson, D. Maltz, Dynamic source routing in ad hoc wireless networks, in: Imielinski, Korth (Eds.), Mobile Computing, Kluwer Academic Publishers, 1996, pp. 153–181.

[82] E. Royer, M. Melliar-Smithy, L. Moser, An analysis of the optimum node density for ad hoc mobile networks, in: Proceedings of the IEEE International Conference on Communications, 2001.

[83] X. Hong, M. Gerla, G. Pei, C.-C. Chiang, A group mobility model for ad hoc wireless networks, in: ACM International Workshop on Modeling and Simulation of Wireless and Mobile Systems (MSWiM'99), 1999.

[84] J. Tian, J. Hahner, C. Becker, I. Stepanov, K. Rothermel, Graph-based mobility model for mobile ad hoc network simulation, in:

[85] L. Hogie, F. Guinand, P. Bouvry, The ad hoc metropolitan ad hoc network simulator, 2005. <http://www-lih.univ-lehavre.fr/hogie/madhoc>.

[86] J. Yoon, M. Liu, B. Noble, Random waypoint considered harmful, IEEE Infocom'03 (2003).

[87] J. Yoon, M. Liu, B. Noble, Sound mobility models, in: MobiCom'03, 2003.

[88] Q. Zheng, X. Hong, S. Ray, Recent advances in mobility modeling for mobile ad hoc network research, in: ACM-SE 42, Proceedings of the 42nd Annual Southeast Regional Conference, 2004.

[89] C. Tuduce, T. Gross, A mobility model based on WLAN traces and its validation, in: Proceedings of INFOCOM'05, 2005.

[90] M. McNett, G. Voelker, Access and mobility of wireless PDA users, Tech. Rep., Department of Computer Science and Engineering, University of California, San Diego, 2004.

[91] M. Kim, D. Kotz, S. Kim, Extracting a mobility model from real user traces, in: Proceedings of IEEE Infocom'06, 2006.

[92] D. Batacharjee, A. Rao, C. Shah, M. Shah, A. Helmy, Empirical modeling of campus-wide pedestrian mobility: Observation on the USC campus, in: IEEE Vehicular Technology Conference (VTC), 2004.

[93] M. McNett, G.M. Voelker, Access and mobility of wireless PDA users, Tech. Rep. CS2004-0780, UC San Diego, 2004.

[94] K. Maeda, K. Sato, K. Konishi, A. Yamasaki, A. Uchiyama, H. Yamaguchi, K. Yasumoto, T. Higashino, Getting urban pedestrian flow from simple observation: realistic mobility generation in wireless network simulation, in: Proceedings of the 8th ACM/IEEE International Symposium on Modeling, Analysis and Simulation of Wireless and Mobile Systems (MSWiM2005), 2005, pp. 151–158.

[95] F. Karnadi, Z. Mo, K.-C. Lany, Rapid generation of realistic mobility models for VANET, in: WCNC'07, 2007.

[96] M. Piorkowski, M. Raya, A.L. Lugo, P. Papadimitratos, M. Grossglauser, J. Hubaux, TraNS: realistic joint traffic and network simulator for VANETs, in: MobiCom'07, 2007.

[97] R. Baumann, S. Heimlicher, M. May, Towards realistic mobility models for vehicular ad hoc networks, in: 26th Annual IEEE Conference on Computer Communications IEEE INFOCOM 2007, MObile Networks for Vehicular Environments (Infocom MOVE'07), 2007.

[98] S. Eichler, B. Ostermaier, C. Schroth, T. Kosch, Simulation of car-to-car messaging: analyzing the impact on road traffic, in: VANET'06, 2006.

[99] C. Lochert, A. Barthels, A. Cervantes, M. Mauve, M. Caliskan, Multiple simulator interlinking environment for IVC, in: VANET'05, 2005.

[100] J.G. Jetcheva, Y.-C. Hu, S.P. Chaudhuri, A.K. Saha, D.B. Johnson, Design and evaluation of a metropolitan area multitier wireless ad hoc network architecture, in: Fifth IEEE Workshop on Mobile Computing Systems and Applications WMCSA, Monterey, CA, 2003.

[101] E. Huang, W. Hu, J. Crowcroft, I. Wassell, Towards commercial mobile ad hoc network applications: A radio dispatch system, in: Proceedings of the 6th ACM International Symposium on Mobile Ad Hoc Networking and Computing, ACM, Urbana-Champaign, IL, 2005, pp. 355–365.

[102] M. Bechler, W. Franz, L. Wolf, Mobile internet access in FleetNet, in: Proceedings of the 13th Fachtagung Kommunikation in Verteilten Systemen (KiVS 2003), 2003.

Proceedings of the 35th Annual Simulation Symposium, 2002, pp. 337–345.

Jonghyun Kim received his B.S. degree in Electrical Engineering, B.S. degree in computer science from Kangnung National University in 2002, and M.S. degree in electrical and Computer Engineering from University of Delaware in 2005. He is currently pursuing his Ph.D. degree. His research includes protocol development, modeling, simulation, and performance evaluation of urban wireless networks.

Vinay Sridhara received the B.E. degree in Computer Science and Engineering in 1999 from R.V. College of Engineering, Bangalore, India; the M.S. degree in Computer Science from University of Southern California, Los Angeles. He received his Ph.D. degree in Electrical and Computer Engineering in 2007 from University of Delaware, Newark, Delaware. He joined the Corporate Research and Development team at Qualcomm Inc. in 2007 where he is currently a Senior Engineer. At University of Delaware, he worked on models and methodologies for realistic simulations of wireless networks. He is currently involved in design and analysis of next generation wireless local/wide area networks.

Stephan Bohacek received the B.S. in Electrical Engineering from the University of California at Berkeley in 1989. He received the Ph.D. in Electrical Engineering from the University of Southern California in 1999 in Control Theory. He is currently an Assistant Professor in the Department of Electrical and Computer Engineering at the University of Delaware. His research focuses on the design, analysis, and control of data networks. His current interests include congestion control, capacity, and routing for wireless and wireline networks, modeling mobile wireless networks, and cross-layer design for wireless networks.